Thieme

Comparison of Dual- and Single-Source Dual-Energy CT for Diagnosis of Acute Pulmonary Artery Embolism

Vergleich zwischen Dual- und Single-Source-Dual-Energy-CT in der Diagnostik der akuten Lungenarterienembolie

Authors
Bernhard Petritsch, Pauline Pannenbecker, Andreas Max Weng, Simon Veldhoen, Jan-Peter Grunz, Thorsten Alexander Bley, Aleksander Kosmala

Affiliation
Institute of Diagnostic and Interventional Radiology, University Hospital of Würzburg, Würzburg, Germany

Key words
CT-angiography, dual-energy, pulmonary embolism, image quality, radiation dose

received 16.03.2020
accepted 05.08.2020
published online 01.10.2020

Bibliography
Fortschr Röntgenstr 2021; 193: 427–436
DOI 10.1055/a-1245-0035
ISSN 1438-9029

Georg Thieme Verlag KG, Rüdigerstraße 14, 70469 Stuttgart, Germany

Correspondence
Dr. Bernhard Petritsch
Institute of Diagnostic and Interventional Radiology, University Hospital of Würzburg, Oberdürrbacher Str. 6, 97080 Würzburg, Germany
Tel.: ++ 49/9 31/20 13 40 10
Fax: ++ 49/9 31/2 01 63 40 01
Petritsch_B@ukw.de

ZUSAMMENFASSUNG

Ziel Vergleich von Dual-Source-Dual-Energy-CT (DS-DECT) und Split-Filter-Dual-Energy-CT (SF-DECT) hinsichtlich objektiver und subjektiver Bildqualitätsparameter und Dosisexposition bei Patienten mit Verdacht auf eine Lungenarterienembolie (LAE).

Material und Methoden Es wurden 135 Patienten, welche bei Verdacht auf eine LAE eine pulmonale Dual-Energy-CT-Angiografie (CTPA) erhielten, in die retrospektive Studie eingeschlossen. Die Scan-Parameter waren 90/Sn150 kV beim DS-DECT- (n = 68 Patienten) und Au/Sn120 kV beim SF-DECT-System (n = 67 Patienten). Die Jod-Injektionsrate betrug 1400 mg/s in der DS-DECT-Gruppe vs. 1750 mg/s in der SF-DECT. Farbkodierte Jod-Distributionskarten wurden für beide Protokolle berechnet. Es wurden die objektive (CT-Abschwächung im Truncus pulmonalis (HU), Signal-Rausch-Verhältnis (SNR), Kontrast-Rausch-Verhältnis (CNR)) und subjektive Bildqualität (2 Auswerter (R), 5-Punkte-Likert-Skala) sowie Dosisparameter (effektive Dosis, größenspezifische Dosiseinschätzungen (SSDE)) erhoben und verglichen.

Ergebnisse In beiden Gruppen waren alle CTPAs von diagnostischer Qualität. Die subjektive Bildqualität der CTPA wurde in 80,9/82,4 % (R1 / R2) der DS-DECT und in 77,6 %/76,1 % der SF-DECT als gut oder exzellent bewertet. Die Qualität der Jod-Distributionskarten der DS-DECT wurde in 83,8/88,2 % als gut oder exzellent bewertet. Beide Auswerter bewerteten die Qualität der Jod-Distributionskarten der SF-DECT signifikant niedriger ($p < 0,05$), wobei nur in 43,3/46,3 % (R1 / R2) eine gute oder exzellente Qualität vorlag. Die HU-Werte im Truncus pulmonalis waren zwischen beiden Gruppen ähnlich (p = n. s.), während SNR und CNR in der Split-Filter-Gruppe signifikant höher waren ($p < 0,001$; $p = 0,003$). Sowohl die effektive Dosis (2,70 ± 1,32 mSv vs. 2,89 ± 0,94 mSv) als auch die SSDE (4,71 ± 1,63 mGy vs. 5,84 ± 1,11 mGy) waren in der Split-Filter-Gruppe signifikant höher ($p < 0,05$).

Schlussfolgerung Bei Verdacht auf eine Lungenembolie ermöglicht der Split-Filter eine Dual-Energy-Untersuchung an Single-Source-CT-Scannern, ist aber mit einer schlechteren Qualität der Jod-Distributionskarten und einer höheren Dosisexposition vergesellschaftet.

Kernaussagen:

- Der Split-Filter ermöglicht eine Dual-Energy-Datenakquisition an Single-Source-Single-Layer-CT-Scannern.
- Verglichen mit dem untersuchten Dual-Source-Dual-Energy-System ist die pulmonale Split-Filter-Dual-Energy-CT mit einer schlechteren Qualität der Jod-Distributionskarten und einer höheren Dosisexposition vergesellschaftet.
- Sowohl der Split-Filter als auch der Dual-Source-Scanner ermöglichen eine CTPA in diagnostischer Bildqualität.

ABSTRACT

Purpose Comparison of dual-source dual-energy CT (DS-DECT) and split-filter dual-energy CT (SF-DECT) regarding image quality and radiation dose in patients with suspected pulmonary embolism.

Materials and Methods We retrospectively analyzed pulmonary dual-energy CT angiography (CTPA) scans performed on two different CT scanners in 135 patients with suspected pulmonary embolism (PE). Scan parameters for DS-DECT were 90/Sn150 kV (n = 68 patients), and Au/Sn120 kV for SF-DECT (n = 67 patients). The iodine delivery rate was 1400 mg/s in the DS-DECT group vs. 1750 mg/s in the SF-DECT group. Color-coded iodine distribution maps were generated for both protocols. Objective (CT attenuation of pulmonary trunk [HU], signal-to-noise ratio [SNR], contrast-to-noise ratio [CNR]) and subjective image quality parameters (two readers [R], five-point Likert scale), as well as radiation dose parameters (effective radiation dose, size-specific dose estimations [SSDE]) were compared.

Results All CTPA scans in both groups were of diagnostic image quality. Subjective CTPA image quality was rated as good or excellent in 80.9 %/82.4 % (R1 / R2) of DS-DECT scans, and in 77.6 %/76.1 % of SF-DECT scans. For both readers, the image quality of split-filter iodine distribution maps was significantly lower ($p < 0.05$) with good or excellent ratings in only 43.3 %/46.3 % (R1 / R2) vs. 83.8 %/88.2 % for maps from DS-DECT. The HU values of the pulmonary trunk did not differ between the two techniques (p = n. s.), while both the SNR and CNR were significantly higher in the split-filter group ($p < 0.001$; $p = 0.003$). Both effective radiation dose (2.70 ± 1.32 mSv vs. 2.89 ± 0.94 mSv) and SSDE (4.71 ± 1.63 mGy vs. 5.84 ± 1.11 mGy) were significantly higher in the split-filter group ($p < 0.05$).

Conclusion The split-filter allows for dual-energy imaging of suspected pulmonary embolism but is associated with lower iodine distribution map quality and higher radiation dose.

Key points:

- The split-filter allows for dual-energy data acquisition from single-source single-layer CT scanners.
- Compared to the assessed dual-source dual-energy system, split-filter dual-energy imaging of a suspected pulmonary embolism is associated with lower iodine distribution map quality and higher radiation dose.
- Both the split-filter and the dual-source scanner provide diagnostic image quality in CTPA.

Citation Format

- Petritsch B, Pannenbecker P, Weng AM et al. Comparison of Dual- and Single-Source Dual-Energy CT for Diagnosis of Acute Pulmonary Artery Embolism. Fortschr Röntgenstr 2021; 193: 427–436

Introduction

Due to its wide availability, relatively low cost, and very short scan time, computed tomography pulmonary angiography (CTPA) is a crucial imaging method for the diagnosis of pulmonary embolism (PE), which is a common and potentially life threatening disease [1–3]. CT enables timely and accurate diagnosis, which is of high importance to allow treatment for optimizing clinical outcomes [4–6].

Different technical approaches have been developed to increase image quality, gain additional functional information and, ideally, simultaneously reduce the radiation dose. In this context the dual-energy CT (DECT) technique provides images with image impression comparable to standard single-energy scans and additionally allows for various post-processing applications. These are based on the fact that different energy levels allow for visualization of absorption characteristics of different materials with high atomic numbers, such as iodine ($_{53}$I) [7, 8]. Post-processing options include image reconstruction at virtual monoenergetic levels (keV), referred to as virtual monoenergetic images (VMI), and the computation of iodine distribution maps reflecting the pulmonary iodine distribution at the time point of imaging. The dedicated advantages of DECT and possibilities of dual-energy imaging in the context of pulmonary embolism have been extensively discussed in the literature [9–13]. In this context especially the value of monoenergetic low-kV images for improved image quality in low contrast settings, as well as the incremental benefit of iodine distribution maps in the detection of occlusive segmental and sub-segmental pulmonary emboli must be mentioned [5, 14].

Most of the published studies covering dual-energy in the field of acute pulmonary embolism used dual-source (DS) CT scanners, where two X-ray tubes operate simultaneously at different energy levels. However, different CT system vendors provide various technical approaches to derive dual-energy data from single-source scanners (e. g. rapid kVp switching; dual-layer detector; split-filter (SF); sequential acquisition) [15].

Recently, a split-filter (SF) was introduced, which offers the advantage of dual-energy data acquisition from single-source CT systems. Although the principle of the split-filter method was already described in 1980 by Rutt et al., the first clinical scanner became available much later in 2014 [16]. The split-filter consists of a combined gold ($_{79}$Au; 50 µm) and tin ($_{50}$Sn; 600 µm) filter with partial coverage in the z-axis direction (▶ **Fig. 1**). The filter is positioned directly in front of the X-ray beam (120 kVp) and results in a low energy spectrum (Au filtration; mean photon energy 68 keV) and a high energy spectrum (Sn filtration; mean photon energy 86 keV) [17, 18]. To date, it is unclear how the split-filter technique performs compared to well-established dual-source scans in patients with acute pulmonary embolism.

Thus, the purpose of this study was to investigate the image quality and radiation dose of DS-DECT in patients with suspected pulmonary embolism compared to SF-DECT examinations.

Materials and Methods

Study design and patient population

The institutional review board approved this retrospective study and waived the need for individual informed consent. We inclu-

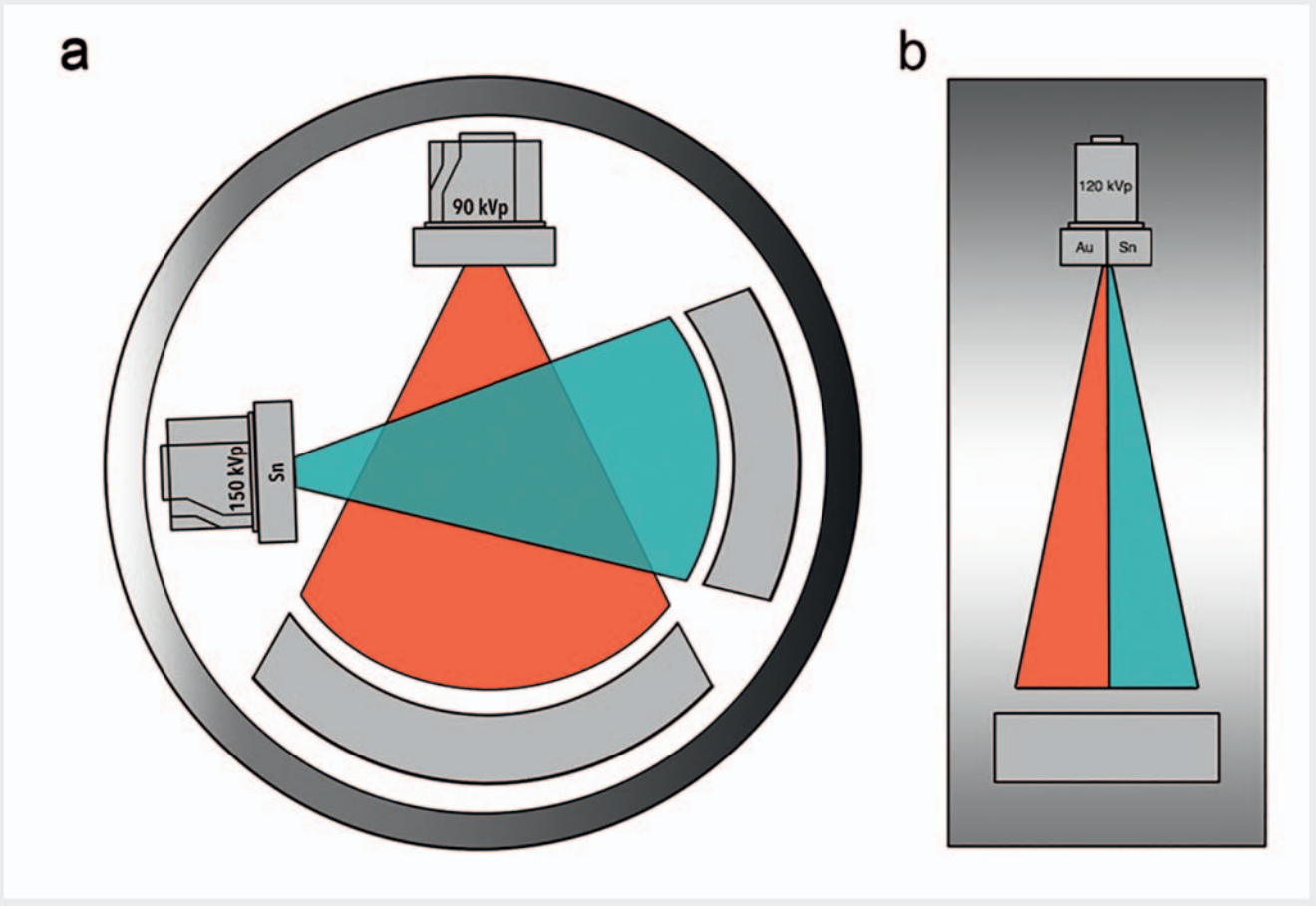

▶ **Fig. 1** Illustration of different technical dual-energy approaches (red = low kV; turquoise = high kV). In the dual-source CT scanner (**a**, frontal view) the dual-energy data is derived from two X-ray tubes (offset by 95°) operating at different energy levels. In the single-source CT scanner (**b**, lateral view) the dual-energy data is derived by an Sn/Au split-filter.

▶ **Abb. 1** Schematische Darstellung der verschiedenen technischen Dual-Energy-Ansätze (rot = Niedrig-kV; türkis = Hoch-kV). Der Dual-Source-CT-Scanner (**a**, frontale Ansicht) generiert die Dual-Energy-Daten aus 2 um 95° versetzte Röntgenröhren. Im Single-Source-CT-Scanner (**b**, seitliche Ansicht) kommt ein Sn/Au-Split-Filter zum Einsatz.

ded and anonymized a total of 140 patients who underwent CT for the workup of suspected acute pulmonary embolism. Of these 140 patients, 70 consecutive patients were imaged with DS-DECT (between March and July 2018) and the other 70 consecutive patients were scanned with SF-DECT (between January and November 2019). Due to severe artifacts, fail of automated lung segmentation software, and previous surgeries, a total of 5 patients (n = 2 in the dual-source group; n = 3 in the split-filter group) were excluded from our study. 135 patients (mean age: 65.3 years ± 15.3 [standard deviation]; range: 18.0–88.0 years) were available for study analysis (▶ **Fig. 2**). The mean age, gender distribution, lateral, anteroposterior, and effective chest diameter as well as the scan length of the patients are shown in ▶ **Table 1**.

CT scan protocols

Dual-source DECT scans were acquired on a 3rd generation 192-slice CT scanner (SOMATOM Force, Siemens Healthcare GmbH, Forchheim, Germany). Split-filter scans were acquired on a 128-slice single-source CT scanner (SOMATOM Definition Edge, Siemens Healthcare GmbH, Forchheim, Germany). The dual-source scanner provides tube energies of 90 kV/Sn150 kV and offers an additional tin ($_{50}$Sn; 600 µm) filter for the high energy tube, whereas the single-source scanner offers the above-described split-filter (TwinBeam Siemens Healthcare GmbH, Forchheim, Germany) for dual-energy acquisitions. Both scanners are equipped with identical single-layer energy-integrating detectors (Stellar, Siemens Healthcare GmbH). A real-time automatic milliampere- second modulation software was used in both scan protocols (CARE Dose 4 D, Siemens Healthcare GmbH). To allow accurate data acquisition from each voxel at both energy levels, the pitch factor was set to 0.55 in dual-source scans and 0.25 in split-filter scans (default settings of the vendor). This resulted in a longer mean scan time in split-filter examinations (2.5 s v s. 9.0 s; $p < 0.05$). The detailed scan parameters for both CT protocols are summarized in ▶ **Table 2**. An iodinated contrast medium (Imeron® 350, Bracco, Konstanz, Germany) was administered by an automated injector (50 ml, flow rate of 4 ml/sec., iodine delivery rate 1400 mg/sec. [dual-source]; 80 ml, flow rate of 5 ml/s, iodine delivery rate 1750 mg/s [split-

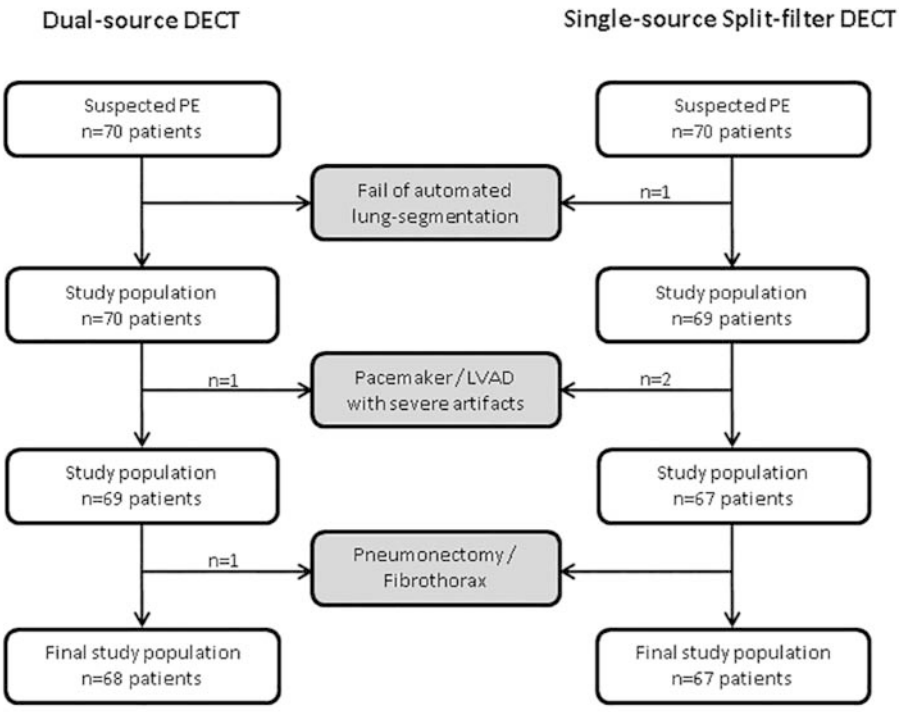

▶ **Fig. 2** Flowchart demonstrating the selection of the study population. 140 patients with suspected pulmonary embolism (PE) were included. Five patients were excluded due to failed automated lung segmentation, severe artifacts (pacemaker, left ventricular assist device [LVAD]), or previous history of pneumonectomy/fibrothorax. A total of 135 patients were available for final evaluation.

▶ **Abb. 2** Flowchart zeigt die Auswahl der Studienpopulation. Einhundertvierzig Patienten mit Verdacht auf Lungenembolie wurden inkludiert. Fünf Scans wurden aufgrund von fehlerhafter automatischer Lungensegmentierung, Artefakten durch Schrittmacher bzw. linksventrikuläre Assist-Devices (LVAD) oder Vorliegen eines Fibrothorax nach Pneumonektomie ausgeschlossen. Einhundertfünfunddreißig Patienten standen zur Auswertung zur Verfügung.

filter]) with an applied trigger attenuation of 120 HU. Both the contrast media delivery rate and dose were tailored to the protocol/scanner used. The 50 ml volume at the 3rd generation dual-source scanner is our well proven routine protocol for dual-energy CTPA. For use of the split-filter protocol, we initially (at time of implementation of the scanner) did a comparison between a volume of 60 ml and 80 ml and found that 80 ml was necessary to compensate for the longer acquisition time in split-filter examinations. Thus, we can ensure an appropriate iodine dose in the pulmonary capillary bed and periphery of the lung to obtain homogeneous iodine distribution maps, while simultaneously maintaining high iodine contrast within the central pulmonary arteries.

For all patients three axial image stacks were reconstructed using iterative image reconstructions (ADMIRE, Siemens Healthcare GmbH) at a strength level of 3 and a medium soft kernel (BR40 / Q40F): Low-energy series (90 kV or Au 120 kVp) and high-energy series (Sn150 kV or Sn 120 kVp) with a slice thickness of 2 mm each; blended series mimicking the image impression of a standard 120 kV examination with a slice thickness of 3 mm. In addition, axial and coronal color-coded iodine distribution maps were reconstructed with a slice thickness of 3 mm using post-processing software (syngo.via VB30A, Siemens Healthcare GmbH) dedicated for dual-energy CTPA evaluation which crops all iodine information except for lung tissue. The smoothing factor was chosen according to the vendor's recommendations (level 4 [dual-source]; level 5 [split-filter]).

Subjective image quality analysis

Two board certified radiologists with 11 years (reader 1 [R1]) and 6 years (reader 2 [R2]) of experience in cardiovascular imaging independently assessed the overall image quality of all CTPA data sets (blended series only) and all color-coded iodine distribution maps according to a five-point Likert scale: 1: no diagnostic image quality, severe artifacts, unsatisfactory CTPA contrast, impossible to assess iodine distribution; 2: poor overall image quality, major artifacts, little CTPA contrast, doubtful applicability of iodine map; 3: fair image quality, minor artifacts, sufficient CTPA contrast, satisfactory iodine map; 4: good overall image quality, minimal artifacts, high CTPA contrast, almost ideal iodine map; 5: excellent overall image quality, no artifacts, excellent CTPA contrast, excellent and homogeneous iodine distribution map. Both readers were blinded to the acquisition technique.

Objective image quality analysis

The mean CT attenuation (Hounsfield units [HU]) in the venous inflow tract (superior vena cava), the pulmonary vasculature (main pulmonary trunk, right lower lobe artery, left upper lobe artery),

▶ **Table 1** Demographic data of patients with suspected pulmonary embolism.

▶ **Tab. 1** Demografische Daten der Patienten mit Verdacht auf eine Lungenembolie.

	Dual-Source-DECT	Split-Filter-DECT	p-Value
patients (n)	68	67	n/a
age (± SD) [years]	64.1 (± 16.0)	66.5 (± 14.6)	n. s.
male (n)/female (n)	40/28	37/30	n/a
scan length (± SD) [mm]	315 (± 33)	308 (± 39)	< 0.001
scan time (± SD) [sec.]	2.49 (± 0.26)	8.99 (± 1.13)	< 0.001
lateral chest diameter (± SD) [cm]	36.4 (± 5.4)	34.7 (± 4.7)	0.042
ap chest diameter (± SD) [cm]	26.7 (± 4.1)	25.2 (± 3.6)	0.021
effective chest diameter (± SD) [cm]	31.1 (± 4.2)	29.5 (± 3.8)	0.015
pulmonary embolism (n)	14	8	n/a

DECT = dual-energy computed tomography; ap = anteroposterior; sec. = seconds; n. s. = not significant.

and the descending aorta was assessed by another reader (1 year of CT imaging experience) using a circular region of interest (ROI) in the 3-mm blended image series. In addition, muscle density was measured within the erector spinae muscles. All ROIs were formed as large as anatomically possible. Subsequently, the signal-to-noise ratio (SNR) and contrast-to-noise ratio (CNR) were calculated as follows:

$$\text{SNR} = \frac{\text{ROI vessel (HU)}}{\text{Image noise vessel (SD of HU)}}$$

$$\text{CNR} = \frac{\text{ROI vessel (HU)} - \text{ROI muscle (HU)}}{\text{Image noise vessel (SD of HU)}}$$

Radiation exposure

The dose-length product (DLP) and the volume computed tomography dose index (CTDIvol) were recorded from the dose report generated by the CT scanner. A conversion factor of 0.018 mSv/mGycm was applied for estimation of the effective radiation dose. In addition, to account for differences in patient habitus, size-specific dose estimations (SSDEs) were calculated as described previously [19].

Statistical analysis

All statistical analyses were performed using dedicated statistical software (SPSS Statistics for windows, version 25, IBM); p-values < 0.05 were considered statistically significant. The Mann-Whitney U test was used for comparison of continuous variables (presented as means ± standard deviations). Subjective image ratings (Likert scale) are presented as absolute numbers and frequencies.

▶ **Table 2** Applied dual-energy scan protocols.

▶ **Tab. 2** Parameter der verwendeten Dual-Energy-Scan-Protokolle.

	Dual-Source-DECT	Split-Filter-DECT
scan mode	dual-source dual-energy	single-source dual-energy
collimation	2 × 96 × 0.6 mm (z-flying focal spot) both detectors	64 × 0.6 mm (z-flying focal spot)
dual-energy FOV	35.3 cm	50.0 cm
rotation time [s]	0.25 s	0.28 s
pitch	0.55	0.25
automatic tube current modulation (CARE Dose 4 D, Siemens)	on	on
automatic tube potential control (CARE kV, Siemens)	off	off
tube potential (ref.) [kV]	90/Sn 150 kV on tube A/B	120 kV with Au/Sn filter
tube current time product (ref.) [mAs]	60/46 mAs on tube A/B	211 mAs

DECT = dual-energy computed tomography; Au = gold; Sn = tin.

To compare Likert scale ratings, the Mann-Whitney U test was used as proposed earlier [20]. The inter-reader reliability for subjective ratings of image quality was evaluated using kappa statistics. Furthermore, the percentage of agreement (both readers gave the same rating) was calculated for the different comparisons.

Results

Pulmonary embolism was diagnosed in 14 of 68 patients (20.6 %) in the dual-source group and in 8 of 67 patients (11.9 %) in the split-filter group.

Subjective image quality

The inter-reader reliability of CTPA and iodine distribution map image quality was excellent in the dual-source group (linear-weighted $\kappa = 0.913$ with $p < 0.001$, 95 % CI 0.819–1.000; $\kappa = 0.880$ with $p < 0.001$, 95 % CI 0.780–0.979) and good in the split-filter group ($\kappa = 0.866$ with $p < 0.001$, 95 % CI 0.762–0.969; $\kappa = 0.824$ with $p < 0.001$, 95 % CI 0.716–0.931). Details are given in ▶ **Table 3**.

All CTPAs in both groups were of diagnostic image quality. The CTPA image quality was rated as good (= 4) or excellent (= 5) in 80.9 %/82.4 % (R1 / R2) of DS-DECT scans. For both readers, the subjective image quality of SF-DECT was significantly reduced compar-

▶ **Table 3** Data for subjective image quality of blended dual-energy CTPA **a** and color-coded iodine distribution maps **b**.

▶ **Tab. 3** Subjektive Bildqualitätsparameter der gemischten pulmonalen Dual-Energy-CT-Angiografie **a** und der farbkodierten Jod-Distributionkarten **b**.

a				
CTPA	**Dual-Source-DECT**		**Split-Filter-DECT**	
Likert scale	*reader 1*	*reader 2*	*reader 1*	*reader 2*
5	45 (66.2 %)	46 (67.6 %)	31 (46.3 %)	28 (41.8 %)
4	10 (14.7 %)	10 (14.7 %)	21 (31.3 %)	23 (34.3 %)
3	10 (14.7 %)	10 (14.7 %)	10 (14.9 %)	11 (16.4 %)
2	3 (4.4 %)	2 (2.9 %)	5 (7.5 %)	5 (7.5 %)
1	–	–	–	–
agreement	95.6 %		89.7 %	
reliability	κ = 0.913		κ = 0.866	
b				
iodine map	**Dual-Source-DECT**		**Split-Filter-DECT**	
score	*reader 1*	*reader 2*	*reader 1*	*reader 2*
5	34 (50.0 %)	34 (50.0 %)	8 (11.9 %)	7 (10.4 %)
4	23 (33.8 %)	26 (38.2 %)	21 (31.3 %)	24 (35.8 %)
3	7 (10.3 %)	4 (5.9 %)	18 (26.9 %)	16 (23.9 %)
2	3 (4.4 %)	3 (4.4 %)	7 (10.4 %)	7 (10.4 %)
1	1 (1.5 %)	1 (1.5 %)	13 (19.4 %)	13 (19.4 %)
agreement	92.6 %		85.3 %	
reliability	κ = 0.880		κ = 0.824	

Image scores: 5 = excellent; 1 = not diagnostic. Values of image quality are given as frequencies (n) and relative percentage (%) in parentheses. Values of agreement are given as percentage (%). Reliability is given as linear weighted kappa value. CTPA = computed tomography pulmonary angiography; DECT = dual-energy computed tomography.

ed to DS-DECT with good or excellent ratings in 77.6 %/76.1 % (R1 / R2) of the scans ($p < 0.05$ for both readers) (▶ **Table 3a**).

Iodine distribution map image quality was rated as good or excellent in 83.8 %/88.2 % (R1 / R2) of DS-DECT scans (▶ **Fig. 3, 4**). For both readers, the subjective image quality of split-filter iodine distribution maps was significantly lower with good or excellent ratings in only 43.3 %/46.3 % (R1 / R2) of the scans ($p < 0.05$ for both readers) (▶ **Table 3b**). There was 1 non-diagnostic iodine distribution map in the dual-source group, compared to 13 non-diagnostic iodine distribution maps in the split-filter group (▶ **Fig. 5**).

Objective image quality

The CT attenuation values within relevant vascular structures, particularly the pulmonary trunk (321.1 ± 126.5 vs. 337.0 ± 110.3), right lower (325.7 ± 120.0 vs. 322.2 ± 130.4) and the left upper lobar artery (328.8 ± 128.7 vs. 297.9 ± 115.2) were similar in both groups (all n. s.). The pulmonary trunk SNR and CNR were both significantly higher in the split-filter group ($p < 0.001$; $p = 0.003$). A detailed overview of the data from all ROI measurements and SNR/CNR calculations is provided in ▶ **Table 4**.

Radiation exposure

The mean effective radiation dose (2.70 ± 1.32 mSv [DS-DECT] vs. 2.89 ± 0.94 mSv [SF-DECT]) and SSDE (4.71 ± 1.63 mGy [DS-DECT] vs. 5.84 ± 1.11 mGy [SF-DECT]) were both significantly higher in the split-filter group ($p < 0.05$). Detailed results of all evaluated radiation dose parameters are given in ▶ **Table 5**.

Discussion

A split-filter offers the possibility to gain dual-energy information from scanners equipped with a single X-ray tube and a standard energy-integrating detector. In this study, we compared this technique with well-established dual-source DECT to assess the impact of a split-filter on both CTPA image quality and dual-energy-derived pulmonary iodine distribution at the time point of imaging by means of iodine distribution maps. To date, only data regarding image quality and associated radiation exposure of split-filter protocols in abdominal as well as in head and neck imaging is available [17, 21–23]. A prior study by May et al., comparing dual- vs. single-source DECT in head and neck imaging (using the same scanner types as in our study), showed similar results to our study in terms of superior image quality of 3rd generation dual-source CT [22]. Other prior split-filter investigations often use a study setting of "single-source split-filter vs. single-source standard protocol" and therefore only offer limited comparability to our study results [17, 21]. To the best of our knowledge, this is the first study to compare the image quality of dual-energy CTPA from a single-source single-layer split-filter scanner vs. a state-of-the-art (3rd generation) dual-source CT-scanner.

Among the existing technologies for dual-energy acquisitions, dual-source scanners offer the highest difference between emission spectra but have the disadvantage of relatively small DE-FOV (limited to the coverage of the smaller detector). Both DS-DECT and SF-DECT use the same single-layer energy-integrating detector, which requires a decision as to whether dual-energy data should be acquired prior to the start of the examination. In comparison, dual-layer ("sandwich") detectors offer the advantage of readily available dual-energy information from every scan on demand. Moreover, because both energy data sets are acquired simultaneously, misregistration of different energy spectra is not a concern and balanced noise between the two energy spectra leads to a lesser decrease in the spectral SNR in the overall system [24]. On the other hand, the time between low and high energy spectrum acquisition in split-filter protocols (approx. 0.5 s) is longer compared to dual-source/dual-layer/rapid kVp switching systems, which typically offer higher temporal resolution in dual-energy co-registration [25].

In patients with suspected pulmonary embolism, CTPA is considered the diagnostic gold standard [1, 26]. The achieved objective CTPA image quality from the split-filter scanner was similar to the image quality derived from the established dual-source approach. In this context attention should be paid to a higher iodine

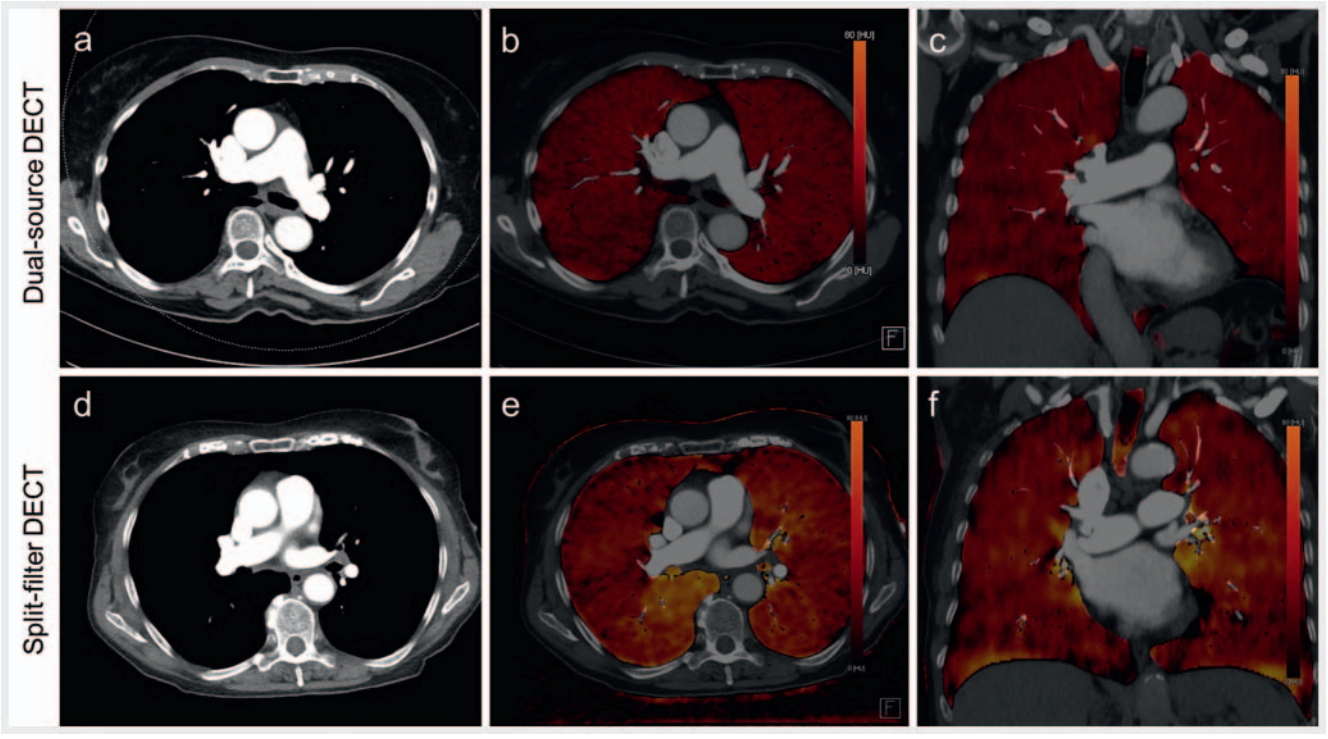

▶ **Fig. 3** Dual-source **a–c** and split-filter **d–e** dual-energy CT (DECT) in patients with ruled out pulmonary embolism. Axial blended virtual 120 kV images **a, d** show proper contrast in the central pulmonary artery vessels. Axial **b, e** and coronal **c, f** reconstructions visualize homogeneous iodine distribution in the color-coded iodine distribution maps (rated as 5 = excellent by both reviewers).

▶ **Abb. 3** Dual-Source **a–c** und Split-Filter **d–e** -Dual-Energy-CT (DECT) bei Patienten mit ausgeschlossener Lungenembolie. Die virtuelle gemischte 120kV-Serie **a, d** zeigt eine regelhafte Kontrastierung der zentralen Lungenarterien. Die axiale **b, e** und koronare **c, f** farbkodierte Jod-Distributionskarte zeigt eine homogene Jodverteilung (von beiden Reviewern mit 5 = exzellent bewertet).

volume as well as delivery rate in the split-filter group, which was chosen to compensate for the significantly longer acquisition time (2.5 s vs. 9.0 s) to still ensure an appropriate iodine dose in the pulmonary capillary bed and periphery of the lung to obtain homogeneous iodine distribution maps, while simultaneously maintaining high iodine contrast within the central pulmonary arteries. However, this may account for the higher vessel opacification, which could have positively influenced objective image quality parameters in terms of a higher CNR.

In this study we demonstrate that the use of a split-filter in CTPA allows for computation of iodine distribution maps from single-source single-layer CT scanners. However, the achieved image quality of iodine distribution maps was significantly lower in the split-filter cohort, with good or excellent results in only < 50 % of the scans. Moreover, there were a total of 13 non-diagnostic iodine distribution maps in the split-filter group, whereas the dual-source iodine distribution maps were of diagnostic quality in all cases except for one single examination. Nearly all of the non-diagnostic iodine distribution maps showed “zebra stripe” artifacts (▶ **Fig. 5**), severely hampering their use for diagnostic considerations. As iodine distribution maps were shown to offer incremental benefits in the detection of occlusive peripheral emboli [5], this issue is especially disadvantageous. There are several potential explanations for the moderate image quality of iodine distribution maps generated by the split-filter scanner in general and the occurrence of typical zebra stripe artifacts in particular. To enable accurate dual-energy data acquisition from each voxel element at both energy levels, the pitch of split-filter protocols is limited to < 0.5 by the vendor and was set to 0.25 (default setting) in our cohort [17, 22]. This is associated with a prolonged scan time which requires a comparatively long breath hold time, which can be problematic in the typical patient with suspected pulmonary embolism, usually presenting with dyspnea. On closer examination, partly obvious, partly subtle respiratory artifacts were visible in all patients presenting with zebra stripe artifacts in our split-filter group. These artifacts usually do not compromise interpretation of conventional CTPA images. However, due to the much greater susceptibility of dual-energy-based iodine distribution maps to even subtle alterations of lung density caused by respiratory motion, the interpretation of iodine distribution maps can be severely impaired by the resulting distinct artifacts [27]. Moreover, compared to dual-source scanners, the single-source approach offers relatively limited spectral separation [18].

We observed a difference in incidence of PE between the two groups in favor of the dual-source group. Possible explanations include the fact that reduced subjective image quality in SF-DECT scans might have had some (most probably minor) impact on PE diagnosis. Furthermore, more liberal patient preselection by the referring colleagues during the time period of split-filter acquisition should also be considered.

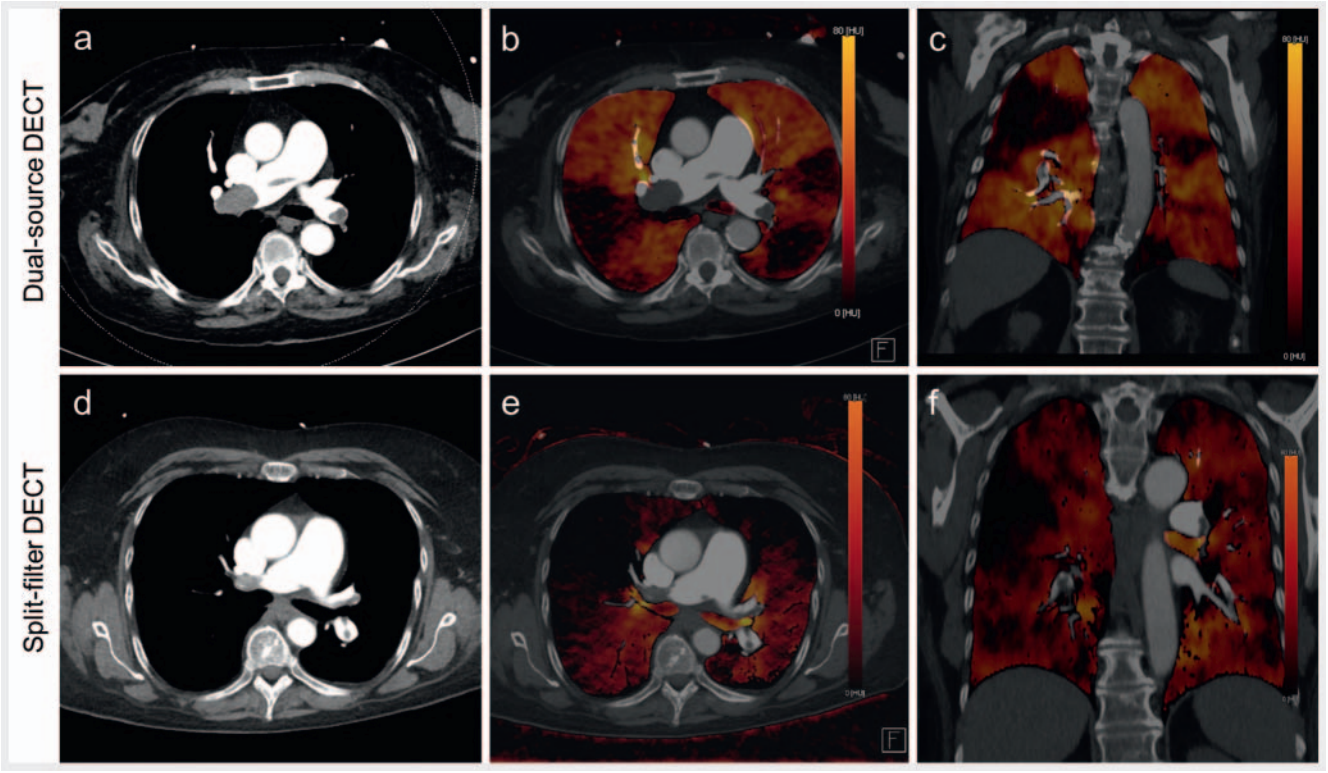

▶ **Fig. 4** Dual-Source **a–c** and split-filter **d–e** dual-energy CT (DECT) in patients with pulmonary embolism. Axial blended virtual 120 kV images **a, d** demonstrate central PE. Axial **b, e** and coronal **c, f** reconstructions visualize the corresponding bilateral wedge-shaped perfusion defects in the color-coded iodine distribution maps (rated as 5 = excellent by both reviewers).

▶ **Abb. 4** Dual-Source **a–c** und Split-Filter **d–e** -Dual-Energy-CT (DECT) bei Patienten mit Lungenembolie. Die virtuelle gemischte 120 kV-Serie **a, d** zeigt eine zentrale Lungenembolie. Die axiale **b, e** und koronare **c, f** farbkodierte Jod-Distributionskarte zeigt die korrespondierenden beidseitigen Perfusionsdefizite (von beiden Reviewern mit 5 = exzellent bewertet).

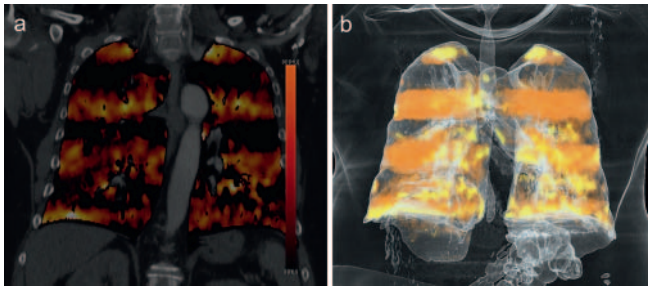

▶ **Fig. 5** Coronal color-coded iodine distribution map **a** and VRT **b** derived from split-filter dual-energy CT (DECT) show severe "zebra stripe" artifacts (images rated as 1 = non-diagnostic by both reviewers).

▶ **Abb. 5** Koronare farbkodierte Jod-Karte **a** und VRT **b** von einer Split-Filter-Dual-Energy-CT (DECT) weisen erhebliche „Zebrastreifen"-Artefakte auf (Bilder von beiden Reviewern mit 1 = nicht diagnostisch bewertet).

With respect to radiation dose, there is an ongoing discussion whether dual-energy imaging is associated with an increased radiation dose or not. Concerning thoracic imaging, there is data from different technical dual-energy approaches which suggests at least dose neutrality [9, 28–32]. In our collective, the split-filter protocol was associated with a modest, but significantly higher radiation dose compared to the dual-source protocol (2.89 vs. 2.70 mSv), despite a significantly shorter scan length and smaller effective chest diameter in the split-filter group. In any case, this is lower than most clinical single-energy routine protocols on still widespread 64-row CT scanners operating at 120 kV [9, 29]. However, taking the risk of gaining non-diagnostic iodine distribution maps and a potential dose penalty into account, the use of a split-filter for diagnostic imaging of a suspected pulmonary embolism should be examined critically.

Our study has several limitations. First, we did not investigate the diagnostic performance of the split-filter protocol vs. dual-source protocol for the detection of a pulmonary embolism. However, taking prior study results into account, we would assume optimized detection of occlusive segmental/sub-segmental pulmonary emboli with the split-filter protocol, if acquired with diagnostic quality [5, 33]. Second, the pulmonary perfused blood volume as a quantitative marker of iodine distribution [34, 35] was not assessed. Third, the number of actual detected pulmonary embolisms was relatively low in our patient collective, which can be primarily explained by liberal patient preselection by the referring colleagues. Fourth, there were small but significant differences in patient habitus and also scan length between the groups. In this context it should be mentioned that the SSDEs

▶ **Table 4** Data for objective image quality of dual-energy CTPA.

▶ **Tab. 4** Objektive Bildqualitätsparameter der pulmonalen Dual-Energy-CT-Angiografie.

	Dual-Source-DECT	Split-Filter-DECT	p-Value
pulmonary trunk			
CT attenuation (HU) (± SD)	321.1 (± 126.5)	337.0 (± 110.3)	n. s.
SNR (± SD)	22.3 (± 8.8)	27.4 (± 7.9)	< 0.001
CNR (± SD)	18.7 (± 8.7)	22.4 (± 7.9)	0.003
right lower lobe			
CT attenuation (HU) (± SD)	325.7 (± 120.0)	322.2 (± 130.4)	n. s.
SNR (± SD)	24.3 (± 9.9)	27.9 (± 15.4)	n. s.
CNR (± SD)	20.5 (± 9.6)	22.8 (± 14.0)	n. s.
left upper lobe			
CT attenuation (HU) (± SD)	328.8 (± 128.7)	297.9 (± 115.2)	n. s.
SNR (± SD)	24.1 (± 10.5)	23.4 (± 12.6)	n. s.
CNR (± SD)	20.1 (± 9.7)	18.6 (± 11.8)	n. s.
descending aorta			
CT attenuation (HU) (± SD)	221.9 (± 62.4)	269.4 (± 68.1)	< 0.001
SNR (± SD)	16.9 (± 6.1)	24.1 (± 6.9)	< 0.001
CNR (± SD)	13.1 (± 5.9)	18.9 (± 6.6)	< 0.001
superior vena cava			
CT attenuation (HU) (± SD)	373.3 (± 194.6)	564.0 (± 324.1)	0.001
SNR (± SD)	8.1 (± 5.5)	10.1 (± 8.4)	0.011
CNR (± SD)	6.5 (± 5.7)	8.5 (± 7.5)	0.004
muscle			
CT attenuation (HU) (± SD)	54.8 (± 9.9)	58.0 (± 10.4)	n.s

CTPA = computed tomography pulmonary angiography; DECT = dual-energy computed tomography; HU = Hounsfield units; SD = standard deviation of HU; SNR = signal-to-noise ratio; CNR = contrast-to-noise ratio; n. s. = not significant.

were still significantly lower in the dual-source group although patient chest diameters were larger. Moreover, subtle differences in image impression allowed identification of the acquisition technique which might have introduced a certain bias. Furthermore, the lower pitch of the split-filter protocol entails a considerable technical limitation of this dual-energy acquisition technology. Last, to compensate for the longer acquisition time in the split-filter study cohort, we used a contrast injection protocol with a higher contrast volume and higher iodine delivery rate, which might have influenced the subjective and objective image quality.

▶ **Table 5** Radiation dose of dual-energy CTPA.

▶ **Tab. 5** Dosisparameter der pulmonalen Dual-Energy-CT-Angiografie.

	Dual-Source-DECT	Split-Filter-DECT	p-Value
CTDIvol (± SD) [mGy]	4.17 (± 1.96)	4.80 (± 1.54)	0.003
DLP (± SD) [mGy*cm]	150.1 (± 73.2)	160.5 (± 52.4)	0.036
Effective dose (± SD) [mSv]	2.70 (± 1.32)	2.89 (± 0.94)	0.036
SSDE (± SD) [mGy]	4.71 (± 1.63)	5.84 (± 1.11)	< 0.001

CTDIvol = volume computed tomography dose index; DLP = dose length product; SSDE = size-specific dose estimates; SD = standard deviation.

Conclusion

The novel split-filter allows for dual-energy data acquisition from single-source single-layer CT scanners. Diagnostic split-filter dual-energy imaging of a suspected pulmonary embolism is feasible but is associated with lower iodine distribution map quality and a higher radiation dose.

CLINICAL RELEVANCE

- The use of a split-filter in CTPA allows for computation of iodine distribution maps from single-source single-layer CT scanners.
- Dual-energy CTPA image quality is diagnostic with both the split-filter and the dual-source technique.
- The diagnostic quality of iodine distribution maps generated by the split-filter scanner is lower compared to those generated by the 3 rd hochgestellt generation dual-source scanner.

Conflict of Interest

Institutional research grand from Siemens Healthcare GmbH.
Bernhard Petritsch: Speaker honorar from Siemens Healthcare GmbH.
Jan-Peter Grunz: Speaker honorar from Siemens Healthcare GmbH.
Thorsten Alexander Bley: Speaker honorar from Siemens Healthcare GmbH and Bracco Imaging GmbH.

References

[1] Tapson VF. Acute pulmonary embolism. N Engl J Med 2008; 358: 1037–1052

[2] Remy-Jardin M, Pistolesi M, Goodman LR et al. Management of suspected acute pulmonary embolism in the era of CT angiography: a statement from the Fleischner Society. Radiology 2007; 245: 315–329

[3] Konstantinides SV, Torbicki A, Agnelli G et al. 2014 ESC guidelines on the diagnosis and management of acute pulmonary embolism. Eur Heart J 2014; 35: 3033–3069, 3069a–3069k

[4] Stein PD, Fowler SE, Goodman LR et al. Multidetector Computed Tomography for Acute Pulmonary Embolism (PIOPEDII). N Engl J Med 2006; 354: 2317–2327

[5] Weidman EK, Plodkowski AJ, Halpenny DF et al. Dual-Energy CT Angiography for Detection of Pulmonary Emboli: Incremental Benefit of Iodine Maps. Radiology 2018; 289: 546–553

[6] Ota M, Nakamura M, Yamada N et al. Prognostic significance of early diagnosis in acute pulmonary thromboembolism with circulatory failure. Hear Vessel 2002; 17: 7–11

[7] McCollough CH, Leng S, Yu L et al. Dual- and Multi-Energy CT: Principles, Technical Approaches, and Clinical Applications. Radiology 2015; 276: 637–653

[8] Johnson TRC. Dual-energy CT: general principles. Am J Roentgenol 2012; 199: 3–8

[9] Petritsch B, Kosmala A, Gassenmaier T et al. Diagnosis of Pulmonary Artery Embolism: Comparison of Single-Source CT and 3rd Generation Dual-Source CT using a Dual-Energy Protocol Regarding Image Quality and Radiation Dose. Rofo 2017; 189: 527–536

[10] Pontana F, Faivre JB, Remy-Jardin M et al. Lung Perfusion with Dual-energy Multidetector-row CT (MDCT). Feasibility for the Evaluation of Acute Pulmonary Embolism in 117 Consecutive Patients. Acad Radiol 2008; 15: 1494–1504

[11] Fink C, Johnson TR, Michaely HJ et al. Dual-energy CT angiography of the lung in patients with suspected pulmonary embolism: initial results. Rofo 2008; 180: 879–883

[12] Bauer RW, Kerl JM, Weber E et al. Lung perfusion analysis with dual energy CT in patients with suspected pulmonary embolism–influence of window settings on the diagnosis of underlying pathologies of perfusion defects. Eur J Radiol 2011; 80: 476–482

[13] Thieme SF, Graute V, Nikolaou K et al. Dual Energy CT lung perfusion imaging–correlation with SPECT/CT. Eur J Radiol 2012; 81: 360–365

[14] Apfaltrer P, Sudarski S, Schneider D et al. Value of monoenergetic low-kV dual energy CT datasets for improved image quality of CT pulmonary angiography. Eur J Radiol 2014; 83: 322–328

[15] Siegel MJ, Kaza RK, Bolus DN et al. White Paper of the Society of Computed Body Tomography and Magnetic Resonance on Dual-Energy CT, Part 1. J Comput Assist Tomogr 2016; 40: 841–845

[16] Rutt B, Fenster A. Split-filter computed tomography: a simple technique for dual energy scanning. J Comput Assist Tomogr 1980; 4: 501–509

[17] Euler A, Parakh A, Falkowski AL et al. Initial Results of a Single-Source Dual-Energy Computed Tomography Technique Using a Split-Filter: Assessment of Image Quality, Radiation Dose, and Accuracy of Dual-Energy Applications in an In Vitro and In Vivo Study. Invest Radiol 2016; 51: 491–498

[18] Almeida IP, Schyns LEJR, Öllers MC et al. Dual-energy CT quantitative imaging: a comparison study between twin-beam and dual-source CT scanners. Med Phys 2017; 44: 171–179

[19] Boone JM, Strauss KJ, Cody DD et al. Size-Specific Dose Estimates In Pediatric and Adult Body CT Examinations: Report No. 204. Am. Assoc. Phys. Medcine, Coll. Park 2011; ISBN: 978-1-936366-08-8

[20] Sullivan GM, Artino AR. Analyzing and Interpreting Data From Likert-Type Scales. J Grad Med Educ 2013; 5: 541–542

[21] Euler A, Obmann MM, Szucs-Farkas Z et al. Comparison of image quality and radiation dose between split-filter dual-energy images and single-energy images in single-source abdominal CT. Eur Radiol 2018; 28: 3405–3412

[22] May MS, Wiesmueller M, Heiss R et al. Comparison of dual- and single-source dual-energy CT in head and neck imaging. Eur Radiol 2018; 29: 4207–4214

[23] Kaemmerer N, Brand M, Hammon M et al. Dual-Energy Computed Tomography Angiography of the Head and Neck With Single-Source Computed Tomography: A New Technical (Split Filter) Approach for Bone Removal. Invest Radiol 2016; 51: 618–623

[24] Große Hokamp N, Maintz D, Shapira N et al. Technical background of a novel detector-based approach to dual-energy computed tomography. Diagn Interv Radiol 2020; 26: 68–71

[25] Siegel MJ, Kaza RK, Bolus DN et al. White Paper of the Society of Computed Body Tomography and Magnetic Resonance on Dual-Energy CT, Part 1: Technology and Terminology. J Comput Assist Tomogr 2016; 40: 841–845

[26] Schoepf UJ, Goldhaber SZ, Costello P. Spiral computed tomography for acute pulmonary embolism. Circulation 2004; 109: 2160–2167

[27] Bauer RW, Schell B, Beeres M et al. High-pitch dual-source computed tomography pulmonary angiography in freely breathing patients. J Thorac Imaging 2012; 27: 376–381

[28] Schenzle JC, Sommer WH, Neumaier K et al. Dual energy CT of the chest: how about the dose? Invest Radiol 2010; 45: 347–353

[29] Bauer RW, Kramer S, Renker M et al. Dose and image quality at CT pulmonary angiography-comparison of first and second generation dual-energy CT and 64-slice CT. Eur Radiol 2011; 21: 2139–2147

[30] Yu L, Primak AN, Liu X et al. Image quality optimization and evaluation of linearly mixed images in dual-source, dual-energy CT. Med Phys 2009; 36: 1019–1024

[31] Sauter AP, Shapira N, Kopp FK et al. CTPA with a conventional CT at 100 kVp vs'. a spectral-detector CT at 120 kVp: Comparison of radiation exposure, diagnostic performance and image quality. Eur J Radiol Open 2020; 7: 100234

[32] Tabari A, Gee MS, Singh R et al. Reducing Radiation Dose and Contrast Medium Volume With Application of Dual-Energy CT in Children and Young Adults. Am J Roentgenol 2020; 214: 1199–1205

[33] Thieme SF, Becker CR, Hacker M et al. Dual energy CT for the assessment of lung perfusion – correlation to scintigraphy. Eur J Radiol 2008; 68: 369–374

[34] Okada M, Kunihiro Y, Nakashima Y et al. Added value of lung perfused blood volume images using dual-energy CT for assessment of acute pulmonary embolism. Eur J Radiol 2015; 84: 172–177

[35] Sueyoshi E, Tsutsui S, Hayashida T et al. Quantification of lung perfusion blood volume (lung PBV) by dual-energy CT in patients with and without pulmonary embolism: preliminary results. Eur J Radiol 2011; 80: e505–e509